

Characterization of Pure and Pb²⁺ ion Doped Methylcellulose Based Biopolymer Electrolyte Films: Optical and Electrical Properties

Omed Gh. Abdullah^{1,2,*}, Shujahadeen B. Aziz^{1,2}, Dlear R. Saber¹

¹ Advanced Materials Research Lab., Department of Physics, College of Science, University of Sulaimani, 46001, Kurdistan Region, Iraq.

² Komar Research Center, Komar University of Science and Technology, 46001, Sulaimani, Kurdistan Region, Iraq.

*E-mail: omedghareb@yahoo.com, omed.abdullah@univsul.edu.iq

Received: 26 July 2018 / Accepted: 22 August 2018 / Published: 5 November 2018

Pb²⁺ ion-conducting biopolymer electrolyte films, based on methylcellulose (MC) were prepared, using the solution cast technique. The effect of Pb²⁺ doping concentration on the optical and electrical properties of host MC are described in this manuscript. Fourier transform infrared (FTIR) spectra indicated the occurrence of complexation between Pb²⁺ and biopolymer host in the synthesis biopolymer-based electrolyte films. Ultraviolet-visible (UV-Vis) spectroscopy accounts for a considerable continuous decline in optical band gap and band tail energy, which attributed to the formation of charge-transfer complex and increasing in the crystalline nature of the polymer electrolyte films, respectively. The dispersion of the refractive index was discussed in term of the single-oscillator model. The frequency-dependent electrical conductivity and dielectric constants of the prepared samples were investigated as a function of temperature and frequency by impedance spectroscopy. Temperature-dependent behavior of the frequency-exponent reveals that the correlated barrier hopping (CBH) model is the most suitable model to describe the conduction mechanism for the present system. The highest value of ion conductivity at ambient temperature was found to be 2.68×10^{-6} S/m for the polymer incorporated with 20 wt.% Lead acetate. The non-Debye type relaxation behaviour has been confirmed by the asymmetric relaxation peak of the imaginary part of the electric modulus. The present biopolymer electrolyte films were specified as promising materials for electrochemical device applications.

Keywords: biopolymer electrolytes; ion conductivity; charge-transfer complex; band structure; conduction mechanism

1. INTRODUCTION

Solid polymer electrolyte materials have attracted considerable attention in view of their potential applications in various electronic and optoelectronic devices such as solar cells, light-emitting diodes, gas sensors, supercapacitors, electrochromic displays, fuel cells, and solid state batteries [1-3]. Solid polymer electrolyte based films overcome several limitations and drawbacks of liquid electrolyte based systems, such as leakage, hazardous gas emission, flammable, and toxicity. High safety, lightweight, low cost, flexibility, ease thin-film formation of solid polymer electrolytes attract the interest of both industrial and academic researchers [4,5].

Optical properties of solid polymer electrolytes have been investigated aiming to achieve remarkable change and tuning the optical properties of host polymer, which are essential for various applications [6-8]; While intensively investigating the electrical properties are aimed to understand the origin and nature of charge transport prevalent in these materials [9]. The optical and electrical properties of solid polymer electrolytes can be suitably tuned by controlling the type and concentration of the salt-additive [10]. In recent years much research activity has been devoted to the synthesis and characterization of solid polymer electrolytes made of various synthetic organic and coordination polymer materials [11-13]. However, these polymers have several disadvantages, such as high cost of fabrication, and not being environmentally-friendly. As an alternative, several renewable natural organic polymers such as hydroxyethyl cellulose [14], cellulose [15], chitosan [16], starch [17], and agar [18] were used as a polymer host for solid polymer electrolytes and showed good ionic conductivity results. Moreover, natural polymers are a well-known biodegradability, renewability, environmentally-friendly, low production cost, and versatile physical and chemical properties [2]. For these reasons, nowadays, the biopolymer electrolyte films have attracted more and more attention [19,20].

Methylcellulose (MC) is a very interesting, natural organic polymer, water-soluble, not toxic, renewable, biodegradable, relatively low-cost, and has good film-forming properties [21,22]. To the best of author's knowledge, there are no results on the optical and electrical properties of MC doped Pb^{2+} ions based biopolymer electrolyte films. Hence, the main objective of this work focuses on the preparation and characterization of biopolymer electrolyte films based on MC as the host polymer for lead ions. It is very important to reveal the optical and electrical parameters of MC incorporation with different filling levels of lead ions, as new material, in order to identify the suitability of the obtained biopolymer electrolyte films for applications towards technology in optoelectronic and electrochemical devices.

2. EXPERIMENTAL SECTION

2.1 Preparation of biopolymer electrolyte

Pure and Pb^{2+} ion doped methylcellulose (MC) based biopolymer electrolyte films were prepared using solution cast technique. MC was obtained from Sigma-Aldrich. A fixed amount of MC

(0.5 g) was first dissolved in 25 ml of distilled water under stirring for 48 hours for complete dissolution of polymer (solution A). On the other hand, different amounts of lead acetate ($\text{Pb}(\text{CH}_3\text{COO})_2$, 99%, Sigma-Aldrich) according to the 5, 10, 15, and 20 wt.% were dissolved separately, each in 5 ml of distilled water (solution B). Biopolymer electrolytes were achieved by mixing solution A and B. The mixture of these solutions were kept on a magnetic stirrer for 30 minutes at room temperature. Now the obtained homogeneous solutions were cast in plastic Petri dishes, and the solvent was allowed to evaporate slowly in a closed container at room temperature for films to form. The dried films were easily peeled off from Petri dishes and coded as BPE-0, BPE-5, BPE-10, BPE-15 and BPE-20 for MC doped with 0, 5, 10, 15, 20 wt.% of Pb^{2+} ions, respectively. The thickness of the obtained free standing-films was in the range of 31 to 38 μm .

2.2 Characterization techniques

The chemical composition of the prepared pure and ion doped MC biopolymer electrolyte films were tested by Fourier transform infrared (FTIR) spectral analysis using (PerkinElmer FT-IR/NIR Frontier spectrometer) infrared spectrometer with a resolution of 1.00 cm^{-1} at room temperature, within the wave number range of $4000\text{-}400\text{ cm}^{-1}$, to detect any possible interaction between cations and the polar functional groups on the backbone of host polymer in the prepared polymer electrolyte films. The optical properties were performed by means of a computerized Ultraviolet-visible (UV-Vis) double beam spectrophotometer (model: Lambda 25) in the wavelength range 190-1100 nm, with 1 nm step, at normal incidence at room temperature. Electrical measurements were carried out to determine the frequency- and temperature-dependence of the electrical conductivity and dielectric response of the samples. The prepared biopolymer electrolyte films were pressed between two aluminum electrodes (2 cm in diameters) to ensure good contact between the electrodes and the electrolyte. The system was installed in a Teflon cell, and the measurements were taken using the precision LCR meter (model: Agilent/HP 4284A), by applying a voltage of 5 mV rms amplitude and varying the frequency from 100 Hz to 1 MHz, and within the temperature range from 30 to 100 $^\circ\text{C}$.

3. RESULTS AND DISCUSSION

3.1 FTIR spectral analysis

In order to identify any possible coordination interaction between the lead acetate salt and the methylcellulose (MC) polymer chains, FTIR measurements were performed. Figure 1 shows the comparison of FTIR spectra of pure and Pb^{2+} ion doped MC as biopolymer electrolyte with 10 and 20 wt.% lead acetate content. It is well known that the observed intense bands at 3446 and 1116 cm^{-1} assigned, respectively, to the stretching vibrations of hydroxyl groups (O-H), and ether groups (C-O-C) of pure MC [23]. The typical characteristic bands of MC appeared at 2908 cm^{-1} indicates the presence of C-H stretching of CH_2 and CH_3 groups. The observed strong bands at 1648 , and 1412 cm^{-1} can be ascribed to the C=O stretching, and C-H bending in CH_2 , respectively [24]. In agreement with

Rangelova *et al.* [25] and Filho *et al.* [26], we also observed characterization bands of pure MC at 1456, 1374, 1316 and 948 cm^{-1} .

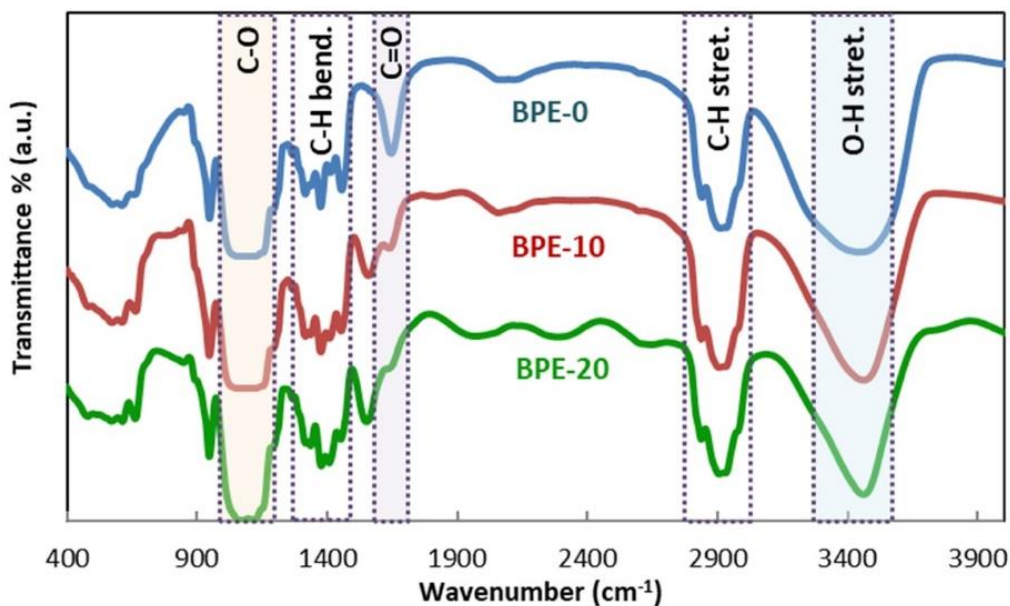


Figure 1. FTIR spectra of BPE-0, BPE-10 and BPE-20 films.

The main difference between the absorption spectra of pure and Pb^{2+} ion doped MC films is the decrease in the intensity and change in the profile of the observed characteristic band of pure MC film. The significant shift of O-H peak from 3446 cm^{-1} for pure MC to 3458 cm^{-1} for 20 wt.% Pb^{2+} ion doped MC, and C=O stretching from 1648 cm^{-1} for pure MC to 1634 cm^{-1} for Pb^{2+} ion doped MC, could be due to the assignment of hydrogen-bonded and the formation of a charge-transfer complex between cations and these polar groups of MC [27-29]. The appearance of the 1552 cm^{-1} peak for biopolymer electrolyte films, and increasing its intensity with increasing lead acetate concentration is mainly due to the presence of acetate ions (CH_3COO^-).

3.2 Ultraviolet-visible spectra analysis

The effects of lead acetate concentration on the optical properties of MC were identified from the optical absorption spectrum, which is the most direct and simplest method of studying the band structure of solids [30]. The UV-Vis absorption spectra at normal incidence of light for the pure and Pb^{2+} doped MC polymer electrolyte films are shown as a function of wavelengths in Fig. 2.

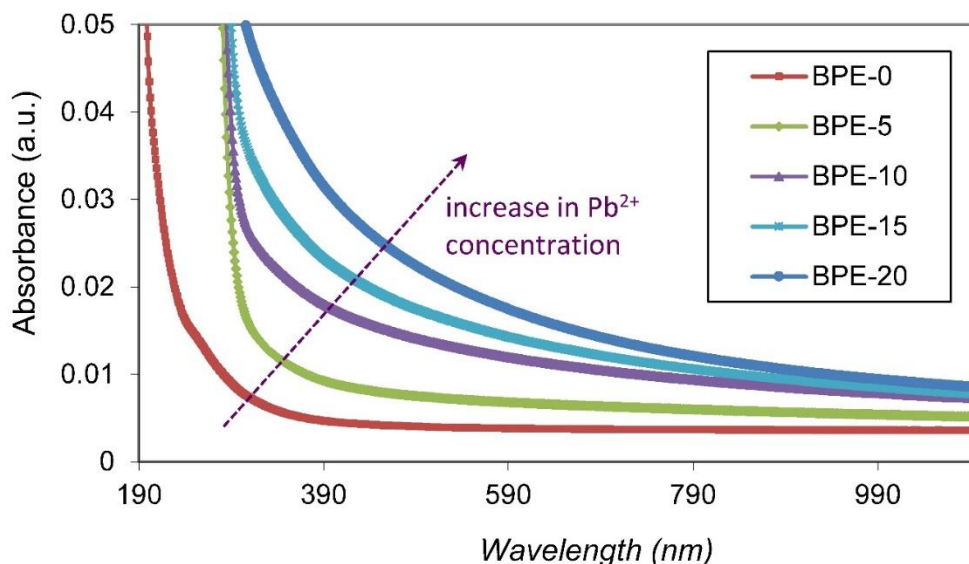


Figure 2. Absorption spectra for pure and Pb²⁺ ion doped MC polymer electrolyte films.

The absorption spectrum of pure MC film is characterized by a sharp absorption edge at 244 nm, which indicates the semi-crystalline nature of MC [31]. The intensity of sharp absorption edge increase and its position shifted towards longer wavelength, by increasing the Pb²⁺ concentration in polymer electrolyte films. This redshift occurs due to the development of strains and the formation of defects, which result in a decrease in the band gap energy of the prepared films [32].

The dependence of optical absorption coefficient on the incident photon energy helps to determine the optical band gap energy and the predominant electron transition involved in the absorption process, by using Tauc’s relation [33]. The optical absorption coefficient (α) is calculated using the relation, $\alpha = 2.303A/d$, where A is the absorbance, and d is the film thickness. The theory of inter-band optical-absorption shows that: the relation between optical absorption coefficient (α) and incident photon energy ($h\nu$) can be expressed as [34,35]:

$$\alpha h\nu = \beta(h\nu - E_g)^\gamma \tag{1}$$

where β is an appropriate constant, h is Plank’s constant, ν is the frequency of radiation, and E_g is the optical energy band gap. Here γ represents an index that can take any of the values 1/2, 3/2, 2 or 3 depending on the type of electronic transition responsible for the optical absorption. To determine the most probable electron transition in the present solid biopolymer electrolyte films, the value of γ has been calculated by taking the natural logarithm and the derivation of Tauc's equation as [36]:

$$\frac{d \ln(\alpha h\nu)}{d h\nu} = \frac{\gamma}{h\nu - E_g} \tag{2}$$

According to this equation, a peak at the value of optical band gap should be observed in the curve of $(d \ln(\alpha h\nu) / d h\nu)$ versus incident photon energy ($h\nu$), as shown in Fig. 3.

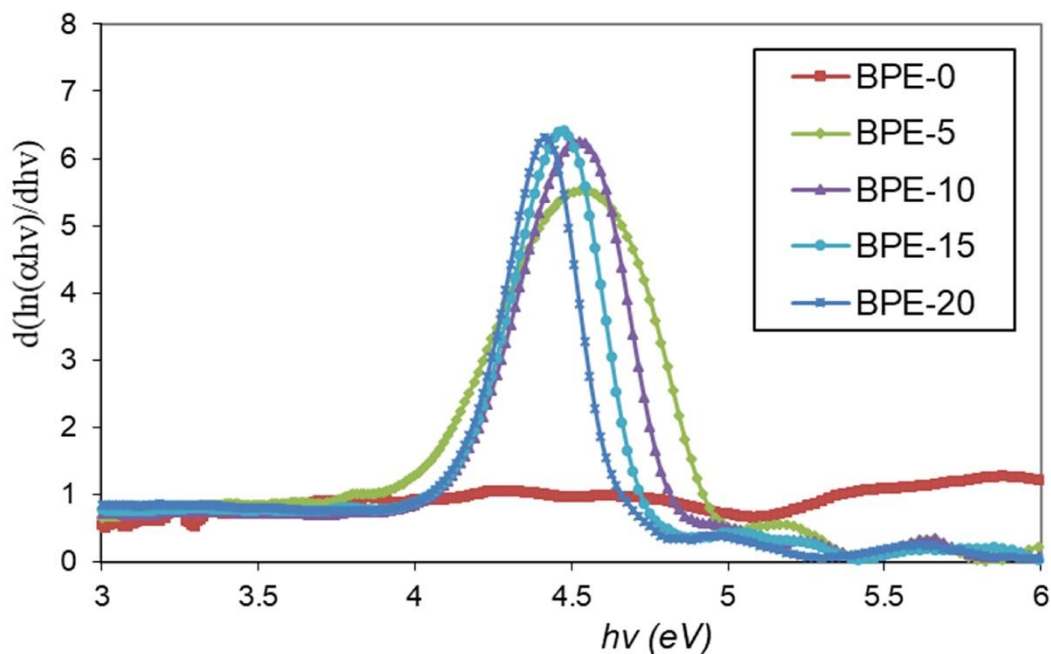


Figure 3. The plot of $(d \ln(\alpha hv) / d hv)$ versus incident photon energy (hv) .

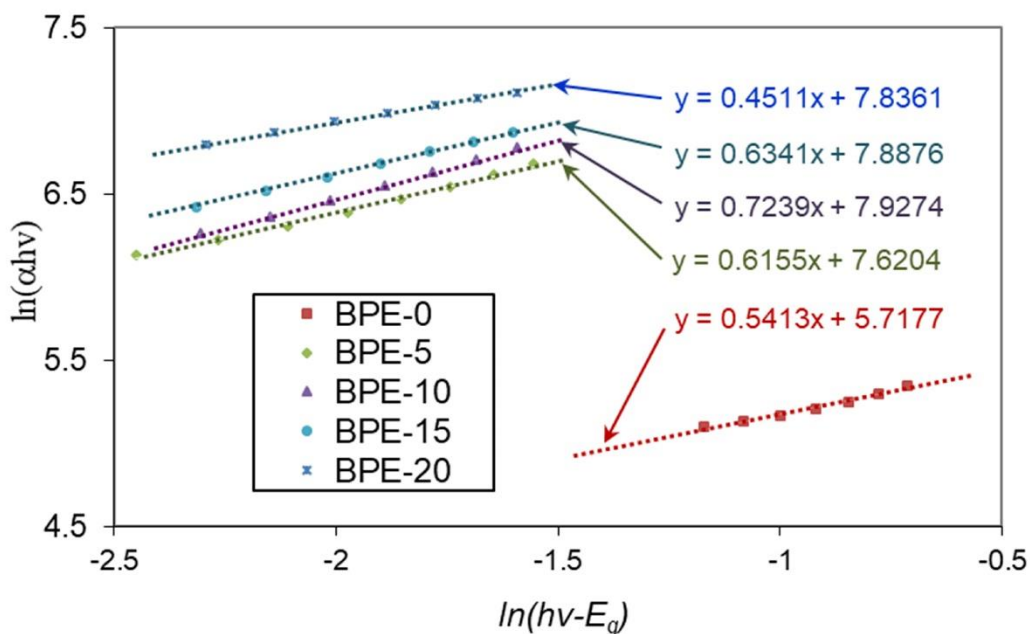


Figure 4. Plot of $\ln(\alpha hv)$ versus $\ln(hv - E_g)$ for pure and Pb^{2+} ion doped MC polymer electrolyte films.

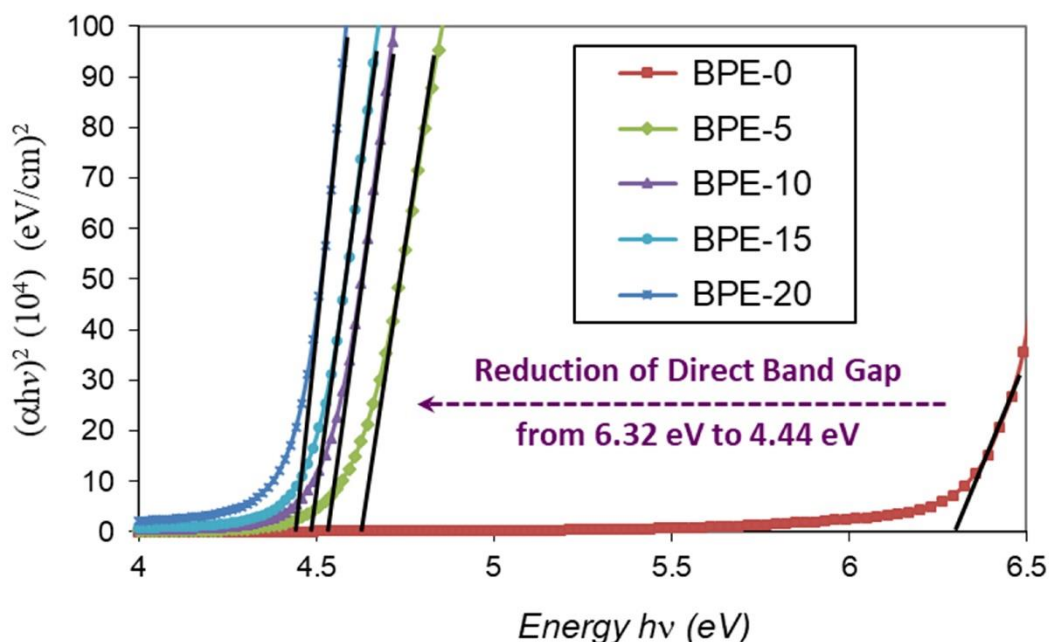


Figure 5. Dependence of $(\alpha hv)^2$ on photon energy (hv) for pure and Pb^{2+} ion doped MC polymer electrolyte films.

The appearance of a peak at a particular energy value gives the approximate value of optical band gap. This approximate value of optical band gaps was used to estimate the value of γ , and hence the nature of electronic transitions [37]. Figure 4 depicted the graph of $\ln(\alpha hv)$ versus $\ln(hv - E_g)$ for pure and Pb^{2+} doped MC biopolymer electrolytes. The value of γ was determined accurately to be in the range (0.45-0.72). Interestingly, this technique provides evidence for the more probable electronic transition in the optical bands. This result indicates clearly, the presence of a direct gap i.e. $\gamma = 0.5$.

The appropriate values of direct optical band gap energy can then be calculated using Tauc's plot. The variation of $(\alpha hv)^2$ with photon energy (hv) for pure MC and MC based biopolymer electrolyte films are presented in Fig. 5. The intercepts of the best fit line on the energy axis give the value of direct allowed optical band gap, which tabulated in Table 1.

Table 1. Optical energy results for MC and its biopolymer electrolyte films.

Samples	E_g (eV)	E_u (eV)
BPE-0	6.32	0.256
BPE-5	4.64	0.196
BPE-10	4.54	0.176
BPE-15	4.49	0.173
BPE-20	4.44	0.178

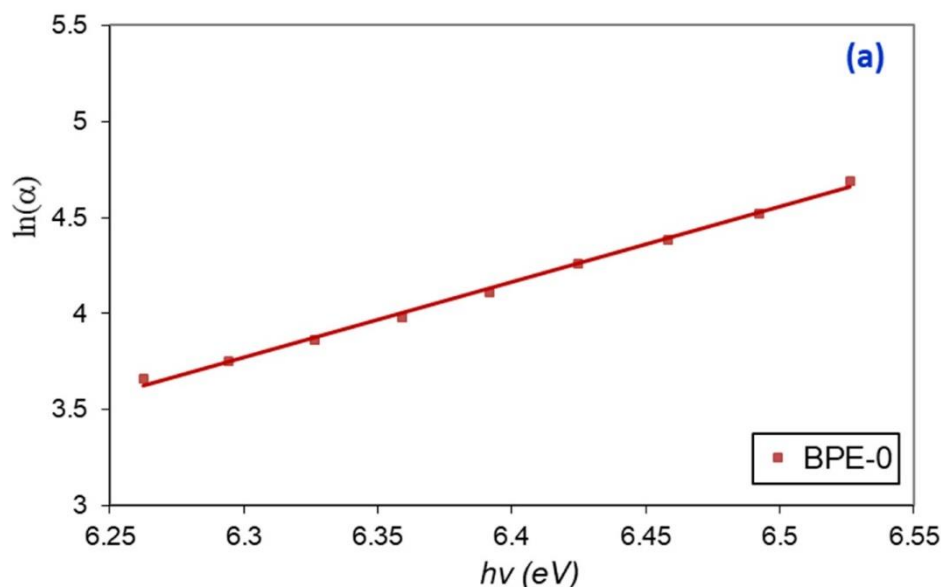
The value of the optical energy gap for the pure MC film was found to be 6.32 eV, which is larger than those published previously by other researchers [38]. For the biopolymer electrolyte films, it was found that E_g is inversely proportional with lead acetate content. The significant decrease in the optical energy band gap is an indication of the increase in the electrical conductivity [39], which may be due to the formation of a charge-transfer complex between lead acetate cation and the hydroxyl groups of the MC polymer chains [40]. This result is very well supported by FTIR analysis (see Fig. 1).

Enhancing the absorption over the Ultraviolet range and low values of energy band gap of the present biopolymer electrolyte films confirm the suitability for applications in optoelectronic device [41].

The absorption coefficient (α) shows an exponential dependence on photon energy ($h\nu$) near the band edge and this dependence is given as Urbach empirical rule [42]:

$$\alpha = \alpha_o \exp\left(\frac{h\nu}{E_u}\right) \quad (3)$$

where α_o is a constant and, E_u is width of the tail of localized state in the band-gap and is known as the Urbach energy. The values of E_u give more detail about the optical behavior of the pure and polymer electrolyte films [39]. Figure 6(a,b) shows the variation of $\ln(\alpha)$ with respect to the photon energy ($h\nu$) at different content of lead acetate in biopolymer electrolyte films. The values of the Urbach energy were determined as the reciprocal of the straight lines slopes shown in Fig. 6, the obtained values have been presented in Table 1.



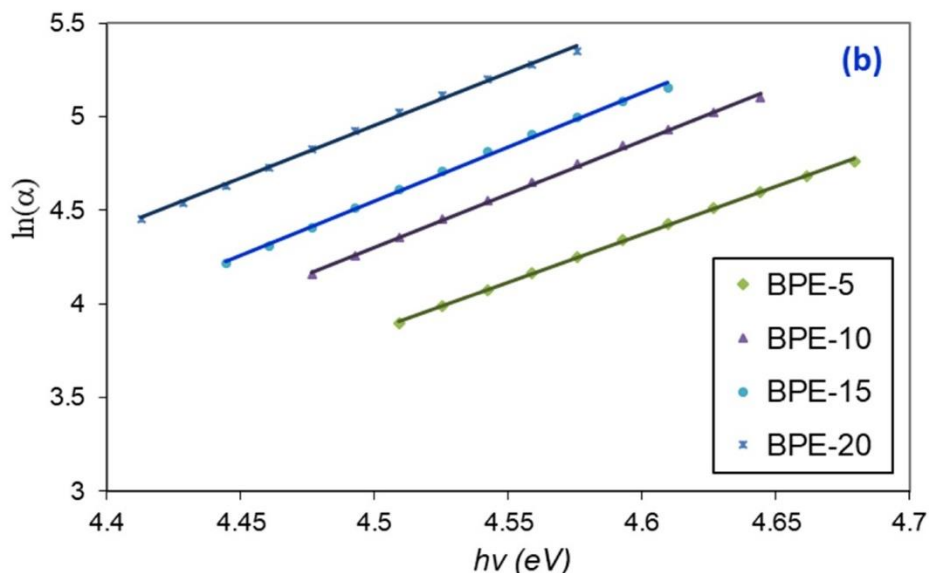


Figure 6. Plot of $\ln(\alpha)$ versus incident photon energy $h\nu$ for: (a) pure MC, and (b) lead ion doped MC biopolymer electrolyte films.

Table 2. The dispersion parameters E_d , E_o for pure and Pb^{2+} doped MC biopolymer electrolyte films.

Samples	E_d (eV)	E_o (eV)	E_o/E_g
BPE-0	1.814	6.265	0.991
BPE-5	0.933	4.703	1.013
BPE-10	1.068	4.683	1.031
BPE-15	1.253	4.668	1.039
BPE-20	1.561	4.676	1.053

It can be seen that the Urbach energy of biopolymer electrolyte films gradually decreases with increase in Pb^{2+} ion content. Thus, the decrease in E_u from 0.25 to 0.17 eV as the lead ion content increases from 0 to 20 wt.% describes the decrease of band tails.

The decrease of band tails may be due to increase in the crystalline nature of the polymer electrolyte. It is well known that the shape of the fundamental optical absorption edge in the exponential region can yield information on the disorder effects [43]. The increase and sharpness of the absorption coefficient in the exponential region for biopolymer electrolyte as shown in Fig. 2, ascribes to the decay of density of the localized states in the optical band gap [44].

The refractive index (n) is the most important optical parameter for optoelectronics application due to its direct relation to the physical, chemical, and molecular properties of materials [45]. The value of n can be determined from reflectance (R) and extinction coefficient ($k = \lambda\alpha/4\pi$) based on the known relationship [46]:

$$n = \frac{1 + R}{1 - R} + \sqrt{\frac{4R}{(1 - R)^2} - k^2} \quad (4)$$

The dispersion of the refractive index of the present biopolymer electrolyte films has been analyzed using the single-oscillator model, which is expressed by the Wemple-DiDomenico relation [47]

$$\frac{1}{(n^2 - 1)} = \frac{E_o}{E_d} - \frac{1}{E_o E_d} (hv)^2 \quad (5)$$

where E_o is the single-oscillator energy, E_d is the dispersion energy. In practice, the dispersion parameters E_o and E_d can be determined from a linear fit parameters of the plot of $1/(n^2 - 1)$ against $(hv)^2$ as shown in Fig. 7.

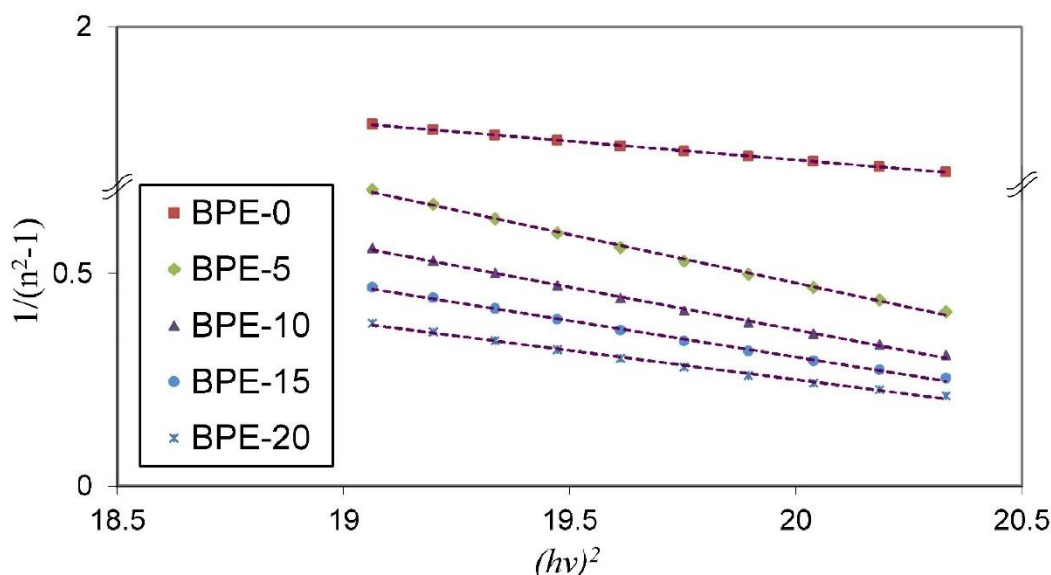


Figure 7. The relation between $1/(n^2 - 1)$ and $(hv)^2$ for prepared films.

The values obtained for the dispersed parameters E_o and E_d are listed in Table 2. The value of oscillator energy E_o is related to the optical energy band gap E_g [48]. Empirically the E_o values of the present films is almost equal to the optical band gap $E_o \approx E_g$ as shown in Table 2. The E_d value is a measure of the strength of inter-band optical transitions, and it was well reported in the literatures that the ordering of the film structure leads to an increase in E_d [49]. This result is also compatible with the results of tail of localized state tabulated in the Table 1.

3.3 Electrical conductivity analysis

Several models are present in the literature to describe the source and nature of charge carriers in polymeric systems, which take into account the particular electronic structure of a given polymer [50]. The measurement of the ac conductivity as a function of frequency, temperature, and composition provides very important information about the nature of the conduction process in materials [51].

For clarity, the plot of the frequency dependence of ac conductivity (σ_{ac}) at different temperatures is displayed in Fig. 8(a,b) for pure and Pb^{2+} ion doped MC samples with 20 wt.% $Pb(CH_3COO)_2$.

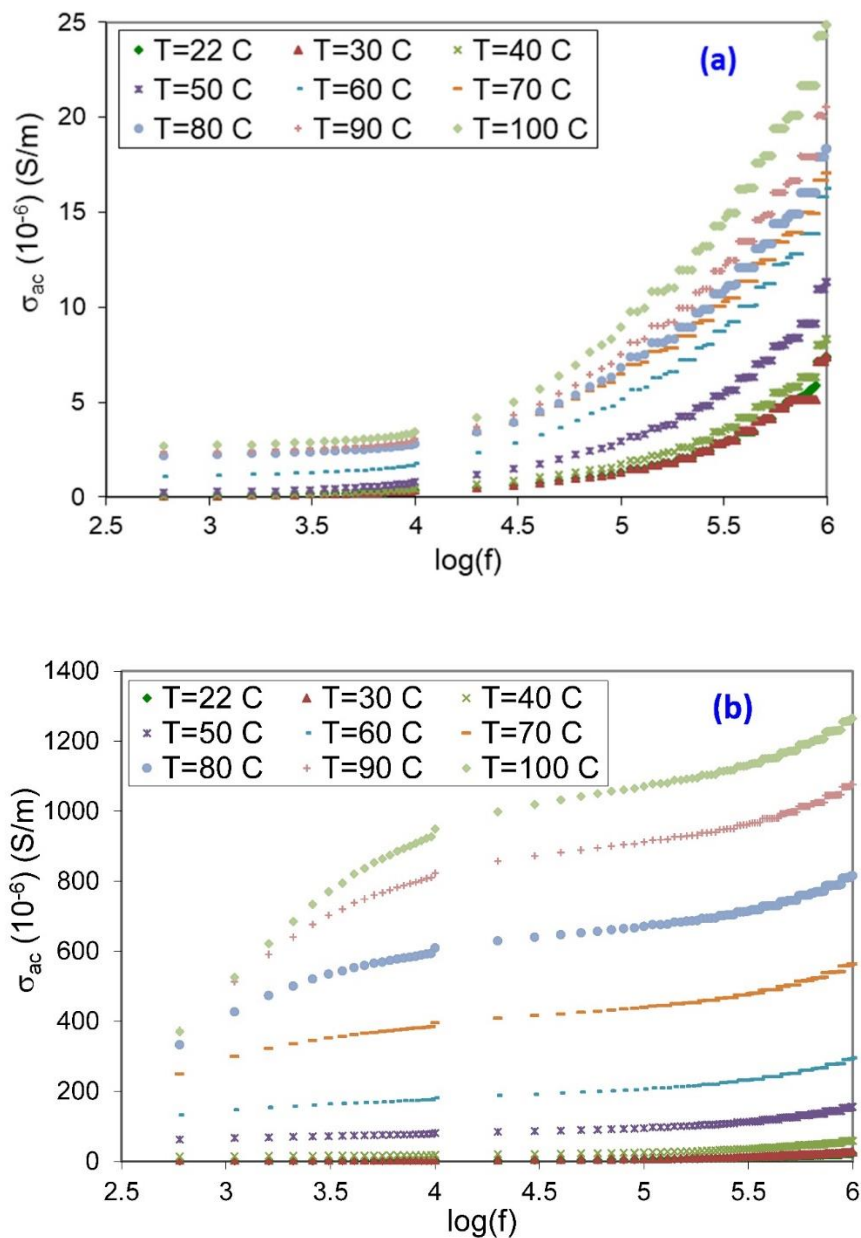


Figure 8. The frequency dependence of the ac conductivity at different temperatures for (a) pure MC, (b) polymer electrolyte doped with 20 wt.% $Pb(CH_3COO)_2$.

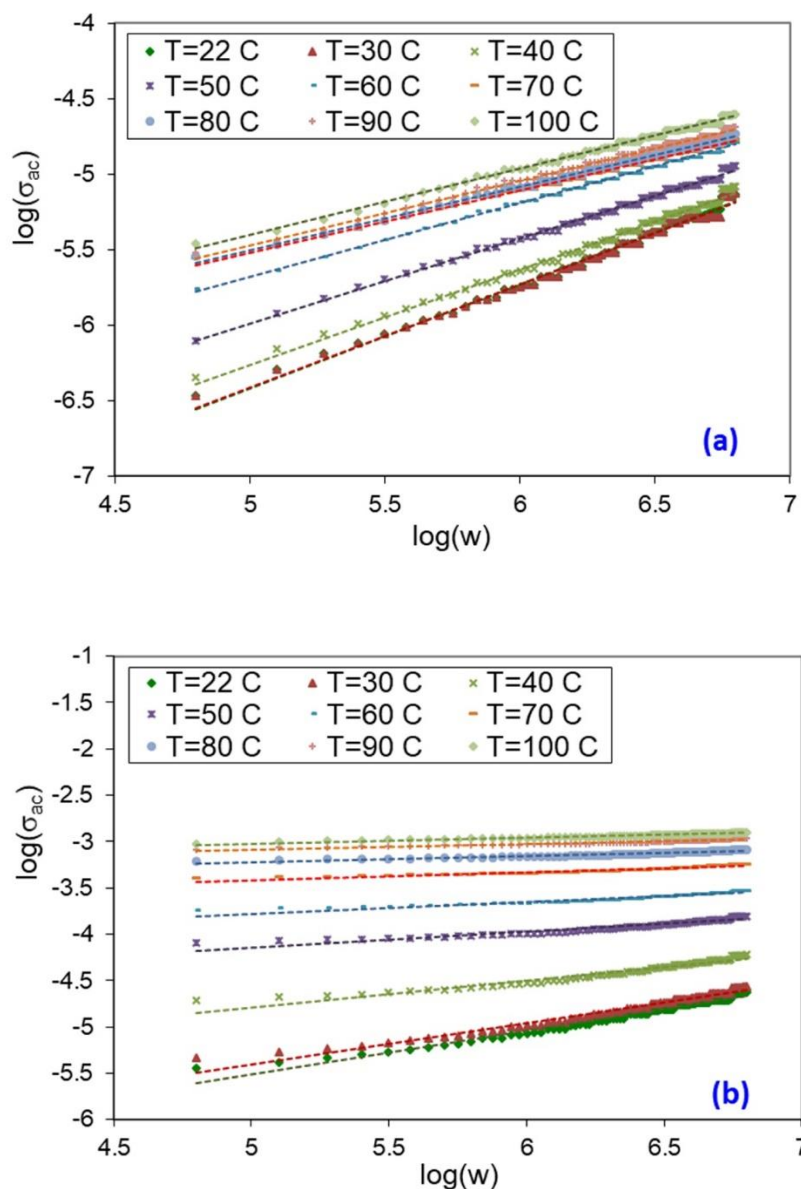


Figure 9. Log-log plot of ac conductivity versus angular frequency for (a) pure MC, (b) polymer electrolyte doped with 20 wt.% $Pb(CH_3COO)_2$ at a different temperature.

The frequency response of the curves indicate the existence of low frequency independent plateau-like region due to dc conductivity (σ_{dc}) and subsequently, the conductivity increases with an increase in frequency, which represents a bulk relaxation phenomenon [52]. Also, it can be seen, each curve shows conductivity dispersion, which is strongly affected by frequency, temperature and Pb^{2+} ion concentration. The value of σ_{ac} increases monotonically with increasing frequency and temperature. This type of behavior reveals that the dominant current transport mechanism could be due to hopping [53]. Thus, the increase of the applied frequency improves the electronic jumps between the localized states; consequently, the ac conductivity increases with increasing frequency [54]. On the other hand, the temperature dependence of the ac conductivity can be explained as follows: the polymer chain mobility increases as the temperature increases, and the fraction of free volume inside

the polymer matrix increases accordingly. This facilitates the segmental motion of the polymer chains and leads to enhancement in σ_{ac} at high temperatures [55]. Moreover, the increase in the ionic conductivity by adding lead salt is attributed to the increase in the number of Pb^{2+} ions as well as their mobility in the polymer host.

It is clear from the curves in Fig. 8 that the ac conductivity has a frequency dependence given by the empirical Jonscher's universal power law [46]

$$\sigma_{ac} = B\omega^s \quad (6)$$

where B is a pre-exponential factor depending on temperature, $\omega = 2\pi f$ is the angular frequency and, s is the dimensionless frequency-exponent, generally less than or equal to unity ($0 < s < 1$). At lower frequencies, ions travel much slower and are able to jump from one available site to another vacant site in the host polymer matrix, and contributes to the dc conductivity. At higher frequencies, the ions perform correlated forward-backward hopping motions on small length scales. The movements are successful when ions jump and stay in the new site. Whereas the movements are unsuccessful hopping if the jumped ion jump back to its initial position [56]. As the ratio of successful to unsuccessful hopping increases, results in more dispersive conductivity at higher frequencies [57].

Table 3. The variation of frequency-exponent (s) with temperature for all samples.

T (K)	(s)				
	BPE-0	BPE-5	BPE-10	BPE-15	BPE-20
295	0.776	0.677	0.445	0.321	0.565
303	0.733	0.672	0.349	0.304	0.554
313	0.695	0.582	0.311	0.194	0.425
323	0.601	0.502	0.261	0.134	0.277
333	0.500	0.426	0.227	0.090	0.209
343	0.446	0.320	0.197	0.066	0.147
353	0.428	0.286	0.172	0.060	0.116
363	0.413	0.254	0.153	0.061	0.098
373	0.407	0.247	0.137	0.053	0.098

To calculate the frequency-exponent (s), the double logarithmic plots of the ac conductivity versus angular frequency at different temperatures for pure MC and MC doped with 20 wt.% lead salt are presented in Fig. 9. It is clear from Fig. 9 that the variation in the $\log(\sigma_{ac})$ is almost linear with the variation in $\log(\omega)$ in the frequency range $4.80 \leq \log(\omega) \leq 6.80$. The frequency-exponent (s) have

been estimated from the slope of the least-square straight-line fits of the experimental data for all temperatures, and is listed as a function of temperature in Table 3. It is evident that the values of s decrease continuously with increasing temperature for both pure and Pb^{2+} ion doped MC films.

Various theoretical models such as the hopping over a barrier (HOB), correlated barrier hopping (CBH), quantum mechanical tunnelling (QMT), small polaron tunneling model (SPT), overlapping large polaron tunneling model (OLPT), etc., have been proposed to explain the conduction mechanism based on the variation of frequency-exponent (s) with temperature. The temperature dependence of the s suggests that the CBH model may be suitable to explain the conduction mechanism in the studied temperature region [9]. In essence, the CBH model considers hopping of carriers between two sites over a potential barriers separating them, rather than tunneling the barrier [58]. According to this model, the values of s has a maximum value at room temperature, and have a tendency to decrease with increasing temperature [53].

The value of activation energies (E_a) have been estimated from the relationship between dc conductivity and temperature, using the Arrhenius relation [52]:

$$\sigma_{dc} = \sigma_o \exp(-E_a/k_B T) \tag{7}$$

where σ_o is a pre-exponential factor, k_B is Boltzmann's constant, and T is temperature in Kelvin. The dc conductivity values were estimated from the extrapolation of the plateau region of ac conductivity spectra shown in Fig. 8.

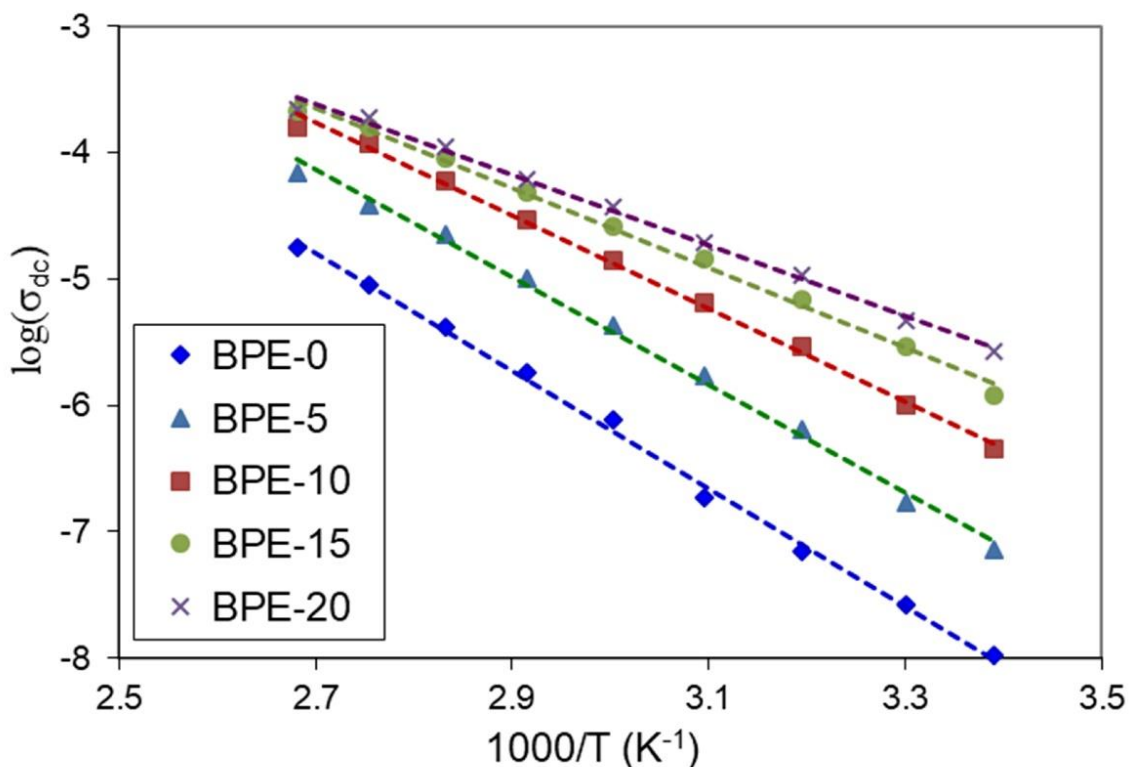


Figure 10. Variation of $\log \sigma_{dc}$ as a function of $1000/T$ for pure and doped MC with $Pb(CH_3COO)_2$.

The conductivity of 20 wt.% Pb^{+2} ion doped film exhibits the highest ion conductivity (2.68×10^{-6} S/m) compared with other electrolyte films, which is due to the increased Pb^{+2} ion within the electrolyte system. The maximum ion conductivity at ambient temperature obtained in this study is higher than that obtained by Krishnakumar et al. [59] (2.264×10^{-7} S/m) for Pb^{+2} ion doped PVA-PEG polymer composite electrolyte films. The variation of dc conductivity versus reciprocal of temperature for present solid polymer electrolyte films, treated as a single straight line region with a single activation energy value, as shown in Fig. 10. The activation energy (E_a) values is extracted from the slope of the plot $\log(\sigma_{dc})$ versus $1000/T$. The variation of E_a as a function of lead ion concentration are depicted in Fig. 11. It is noticed that the value of E_a is inversely proportional to the lead ion content. Therefore, the highest ion content, have the lowest activation energy, and hence maximum dc conductivity.

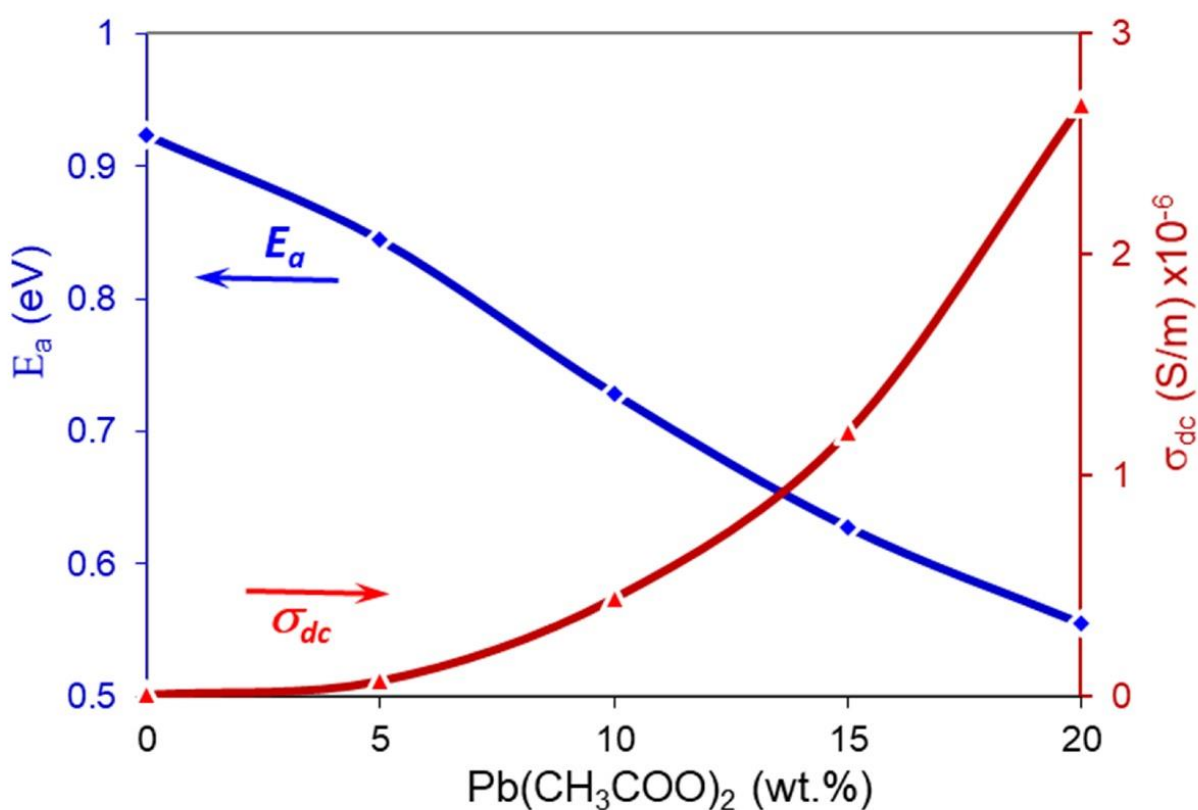


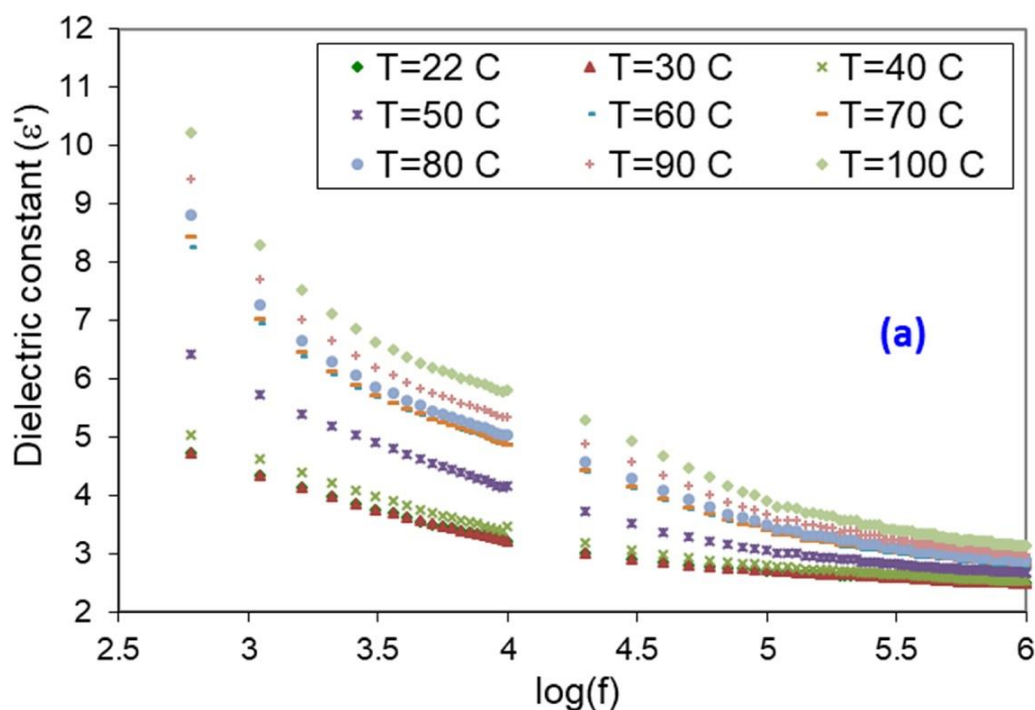
Figure 11. Variation of activation energy and dc-conductivity versus lead salt concentration.

3.4 Dielectric constant analysis

The dielectric polarization in polymer electrolyte systems may be due to several microscopic processes, such as dipole alignment, rotation/motion of the segmental polymer chain, migration of ions, the drift of electrons or holes, and charge injection from the electrodes [31,50]. Methylcellulose

(MC) belong to the group of polyglycans, carrying two hydroxyl side groups (-OH) and one hydroxymethyl side group (-CH₂-OH). These permanent dipolar moments of the attached side groups will be the source of the dielectric relaxation.

Figure 12 shows the frequency-dependence of the dielectric constant (ϵ') at different temperatures for pure and doped MC samples with 20 wt.% Pb(CH₃COO)₂. A high value of ϵ' has been observed in the case of Pb²⁺ ion doped polymer electrolyte films in comparison with the pure MC film. The overall increase in dielectric constant with increasing Pb²⁺ concentration, indicates improvement in the polarizability contributions. Moreover, the dielectric constant (ϵ') decreases with increasing applied frequency at given temperature because the permanent dipoles are no longer able to keep up with changes in the applied electric field, consequently the number of orientational polarization of polar molecules decreases at higher frequencies [9]. It is worth noting that the value of the dielectric constant (ϵ') is also increases with increasing the temperature. This is because the orientation polarization is related to the thermal motion of the molecules [60]. At lower temperatures, the absorbed thermal energy by the polymeric material, at a certain frequency is small, so that a small number of dipoles per unit volume can orient themselves in the direction of the applied electric field [55]. As the temperature increases, the viscosity of the polymeric material is decreased, and the dipoles have enough energy to orient themselves easily in the direction of the applied electric field, and thus the orientation polarization increases, which consequently increases the dielectric constant [60,61].



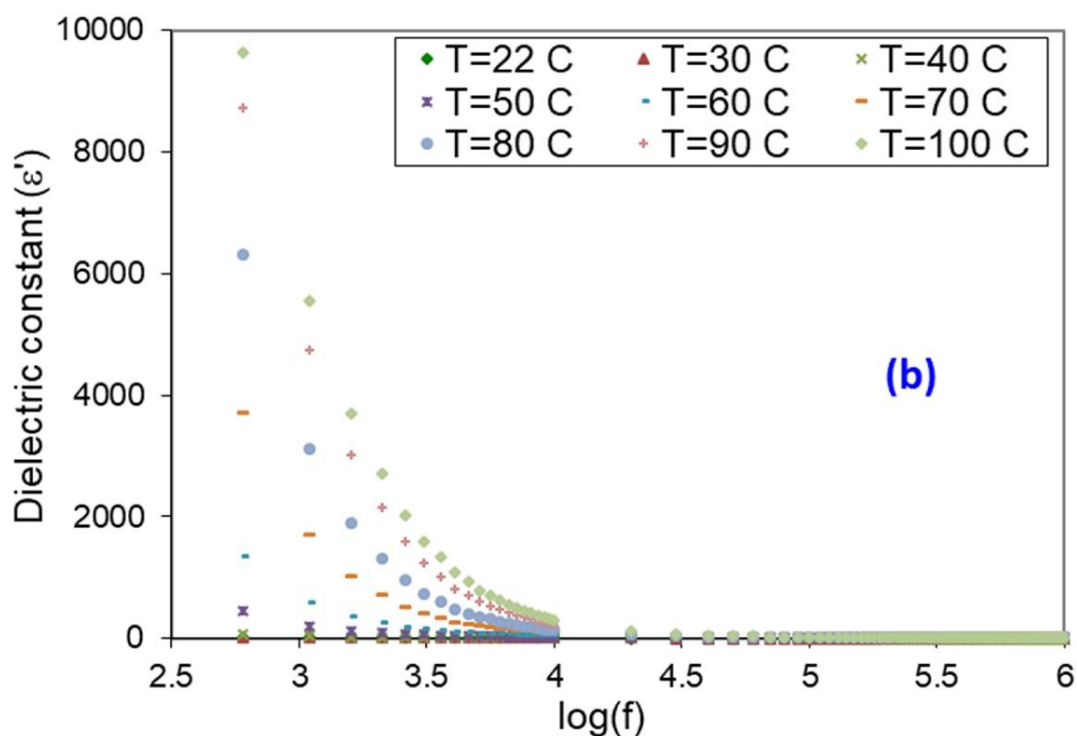


Figure 12. Variation of dielectric constant with frequency at different temperature for (a) BPE-0, and (b) BPE-20.

Based on the obtained results, the optical and dielectric properties of MC can be modified significantly by introducing Pb^{2+} ions. Therefore, $\text{MC}/\text{Pb}(\text{CH}_3\text{COO})_2$ biopolymer electrolyte is a candidate for several industrial and electronic devices with improved the dielectric strength and charge storage capacity.

3.5 Electrical Modulus analysis

The electric modulus (reciprocal quantity of dielectric permittivity), has been extensively used to analyze and interpret the dielectric response caused by charge relaxation, in which the electrode polarization effects are suppressed [62]. The modulus formalism provides wider insights into ion dynamics processes as a function of frequency at a different temperature. Figure 13 showed the frequency-dependence of the real and imaginary parts of the complex electrical modulus, (M' and M''), for 20 wt.% Pb^{2+} ion doped MC (BPE-20), at different temperature.

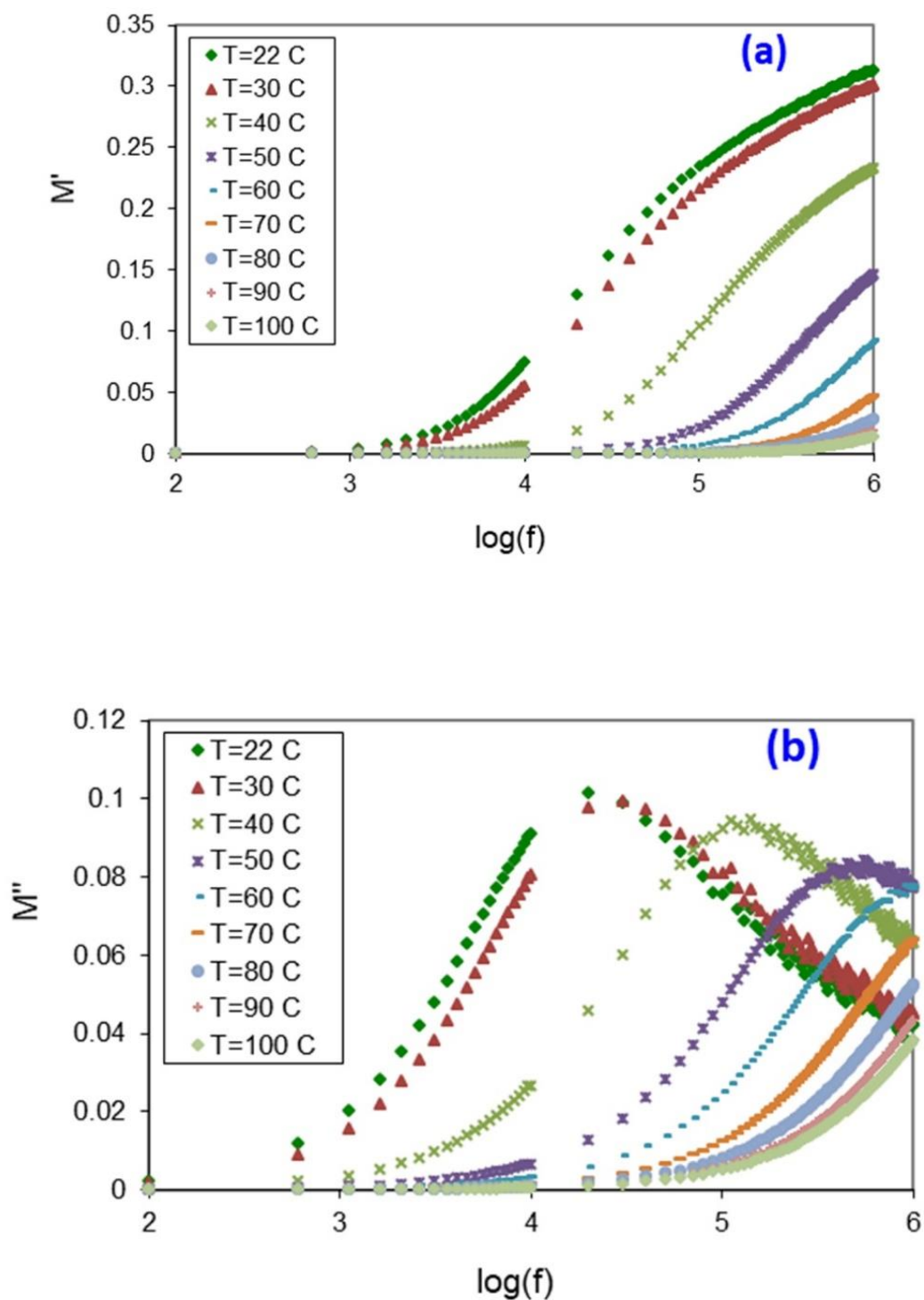


Figure 13. Variation of (a) real and (b) imaginary parts of complex electrical modulus with frequency at different temperature for BPE-20.

The plot of M' displays low value at lower frequencies due to the large value of capacitance associated with the electrodes. The observed dispersion of M' with frequency is ascribed to conductivity relaxation which accompanied by a loss peak in the diagram of M'' versus frequency. The

reduction in M' with increasing temperature is related to the segmental chain motion due to an increase in free volume caused by the thermal expansion [24]. The M'' spectra in Fig. 13-b shows a single relaxation peak that converges at the dispersion region of M' . The asymmetric and broadening in M'' peak is indicative of a non-Debye type relaxation behavior in the present electrolyte system [63]. The observed low frequencies relaxation peak is shifted toward the higher frequencies side with an increase in temperature. This revealed that relaxation time for charge carriers motion decreases with increasing temperature due to the increase in carrier's mobility and dipolar orientation [24].

In polymer electrolyte systems more than one type of polarization mechanism occurs due to interactions between ions and polar groups of the polymer backbone. Thus there were distributions of relaxation time. The study of Argand diagrams (M' vs. M'') at different temperatures can be used to provide insight into the nature of the relaxation processes in the present biopolymer electrolyte system. It was well reported that, if Argand plot shows semicircular behavior, then the relaxation is due to conductivity relaxation process. Otherwise, it is due to viscoelastic relaxation [64].

Figure 14 shows the Argand plots at different temperature for 20 wt.% Pb^{2+} ion doped MC polymer electrolyte film. It can be seen clearly, that the Argand plots of this sample exhibit incomplete semicircular arcs, indicating, non-Debye relaxation, and ion transport occurs due to carrier relaxation process with a single value of relaxation time, at the frequency-domain range [16]. Moreover, it can be seen that with increasing temperature, the relaxation peak shifts toward the origin, confirming the increase in conductivity due to the thermal activation process.

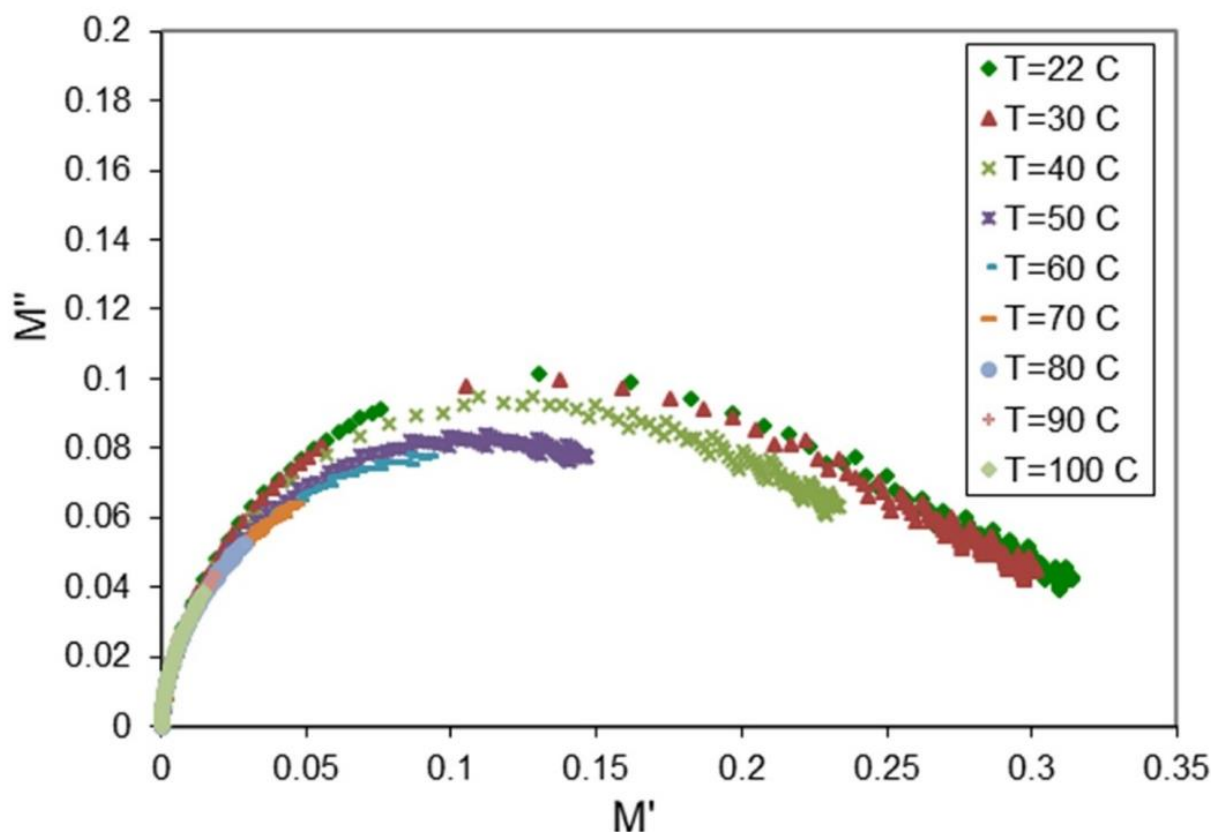


Figure 14. Argand plots spectra at different temperature for BPE-20.

4. CONCLUSION

The eco-friendly biopolymer electrolyte films were prepared by incorporating various compositions of lead acetate with MC biopolymer using the solution cast technique. The dependence of the fundamental optical and electrical parameters of the MC polymer electrolyte on Pb^{2+} ion content was investigated. FTIR studies confirm the complexation due to the interaction of the lead cation with the functional groups on the backbone of host polymer. The increase of optical absorption in the ultraviolet region of this system is due to the excitations of donor electrons to the conduction band at these energies. The direct transition band gap for biopolymer electrolyte films decreases with increasing the Pb^{2+} ion content. This behavior may be associated with the structural changes occurring after the addition of lead acetate salt. The decrease of Urbach energy of polymer electrolyte is obtained upon addition of lead ions, which correlated with the decrease of disorder in the system. The temperature dependence of the frequency-exponent (s) of the present biopolymer electrolyte systems, reveal that correlated barrier hopping (CBH) model is the dominant conduction mechanism in the MC/ $\text{Pb}(\text{CH}_3\text{COO})_2$ system. The maximum ionic conductivity of 2.68×10^{-6} S/m at ambient temperature was observed for the sample containing 20 wt.% $\text{Pb}(\text{CH}_3\text{COO})_2$. The electrical modulus analysis demonstrated a non-Debye type of relaxation process.

ACKNOWLEDGEMENT

The authors gratefully acknowledge the financial support from the Kurdistan National Research Council (KNRC)- Ministry of Higher Education and Scientific Research-KRG, Iraq. The authors would also appreciatively acknowledge the support received from the University of Sulaimani, and the Komar University of Science and Technology for carrying out this work.

References

1. M.S.A. Rani, S. Rudhziah, A. Ahmad and N.S. Mohamed, *Polymers*, 6 (2014) 2371.
2. S.B. Aziz, O.G. Abdullah and M.A. Rasheed, *J. App. Polym. Sci.*, 134 (2017) 44847.
3. T. Hibino, K. Kobayashi, P. Lv, M. Nagao and S. Teranishi, *Bull. Chem. Soc. Jpn.*, 90 (2017) 1017.
4. A.F. Abdulameer, M.H. Suhail, O.G. Abdullah and I.M. Al-Essa, *J. Mater. Sci. Mater. Electron.*, 28 (2017) 13472.
5. O.G. Abdullah, D.A. Tahir and K. Kadir, *J. Mater. Sci. Mater. Electron.*, 26 (2015) 6939.
6. P.A. Tomar, S.M. Yadav and G.R. Gupta, *Polym. Bull.*, 71 (2014) 1349.
7. S.B. Aziz, O.G. Abdullah, A.M. Hussein and H.M. Ahmed, *Polymers*, 9 (2017) 626.
8. H.N. Chandrakala, B. Ramaraj, Shivakumaraiah and Siddaramaiah, *J. Alloys Compd.*, 586 (2014) 333.
9. O.G. Abdullah, Y.A.K. Salman and S.A. Saleem, *J. Mater. Sci. Mater. Electron.*, 27 (2016) 3591.
10. O.G. Abdullah, S.B. Aziz, K.M. Omer and Y.M. Salih, *J. Mater. Sci. Mater. Electron.*, 26 (2015) 5303.
11. N.S. Salleh, S.B. Aziz, Z. Aspanut and M.F.Z. Kadir, *Ionics*, 22 (2016) 2157.
12. T. Yamada, M. Sadakiyo, A. Shigematsu and H. Kitagawa, *Bull. Chem. Soc. Jpn.*, 89 (2016) 1.
13. D. Sheberla, J.C. Bachman, J.S. Elias, C.J. Sun, Y.S. Horn and M. Dinca, *Nat. Mater.*, 16 (2017) 220.

14. G.O. Machado, H.C.A. Ferreira and A. Pawlicka, *Electrochim. Acta*, 50 (2005) 3827.
15. F. Bella, S. Galliano, M. Falco, G. Viscardi, C. Barolo, M. Gratzel and C. Gerbaldi, *Green Chem.*, 19 (2017) 1043.
16. S.B. Aziz, O.G. Abdullah, S.A. Hussein and H.M. Ahmed, *Polymers*, 9 (2017) 622.
17. R.I. Mattos, C.E. Tambelli, J.P. Donoso and A. Pawlicka, *Electrochim. Acta*, 53 (2007) 1461.
18. E. Raphael, C.O. Avellaneda, B. Manzolli and A. Pawlicka, *Electrochim. Acta*, 55 (2010) 1455.
19. A.S. Samsudin, H.M. Lai and M.I.N. Isa, *Electrochim. Acta*, 129 (2014) 1.
20. S.B. Aziz, O.G. Abdullah, M.A. Rasheed and H.M. Ahmed, *Polymers*, 9 (2017) 187.
21. T. Mekonnen, P. Mussone, H. Khalil and D. Bressler, *J. Mater. Chem. A*, 1 (2013) 13379.
22. A.S. Samsudin, E.C.H. Kuan and M.I.N. Isa, *Int. J. Polym. Anal. Charact.*, 16 (2011) 477.
23. N.A.N. Aziz, N.K. Idris and M.I.N. Isa, *Int. J. Polym. Anal. Charact.*, 15 (2010) 319.
24. O.G. Abdullah, R.R. Hanna and Y.A.K. Salman, *J. Mater. Sci. Mater. Electron.*, 28 (2017) 10283.
25. N. Rangelova, L. Radev, S. Nenkova, I.M.M. Salvado, M.H.V. Fernandes and M. Herzog, *Cent. Eur. J. Chem.*, 9 (2011) 112.
26. G.R. Filho, R.M.N. Assuncao, J.G. Vieira, C.S. Meireles, D.A. Cerqueira, H.S. Barud, S.J.L. Ribeiro and Y. Messaddeq, *Polym. Degrad. Stabil.*, 92 (2007) 205.
27. S.B. Aziz, M.A. Rasheed, S.R. Saeed and O.G. Abdullah, *Int. J. Electrochem. Sci.*, 12 (2017) 3263.
28. M. Hema, S. Selvasekarapandian, D. Arunkumar, A. Sakunthala and H. Nithya, *J. Non-Cryst. Solids*, 355 (2009) 84.
29. S.B. Aziz, O.G. Abdullah, D.R. Saber, M.A. Rasheed and H.M. Ahmed, *Int. J. Electrochem. Sci.*, 12 (2017) 363.
30. K. Kesavan, C.M. Mathew, S. Rajendran and M. Ulaganathan, *Mater. Sci. Eng. B*, 184 (2014) 26.
31. M.F.H. Abd El-Kader and H.S. Ragab, *Ionics*, 19 (2013) 361.
32. S.S. Nair, M. Mathews and M.R. Anantharaman, *Chem. Phys. Lett.*, 406 (2005) 398.
33. O.G. Abdullah, S.B. Aziz and M.A. Rasheed, *Results Phys.*, 6 (2016) 1103.
34. E.M. El-Menyawy, A.A.A. Darwish and I.T. Zedan, *Opt. Laser Technol.*, 79 (2016) 158.
35. A.P. Indolia and M.S. Gaur, *J. Polym. Res.*, 20 (2013) 43.
36. F.F. Muhammad and K. Sulaiman, *Measurement*, 44 (2011) 1468.
37. O.G. Abdullah, *J. Mater. Sci. Mater. Electron.*, 27 (2016) 12106.
38. H.S. Ragab and M.F.H.A El-Kader, *Phys. Scr.*, 87 (2013) 025602.
39. R.M. Radwan, *J. Phys. D: Appl. Phys.*, 40 (2007) 374.
40. J. Rozra, I. Saini, A. Sharma, N. Chandak, S. Aggarwal, R. Dhiman and P.K. Sharma, *Mater. Chem. Phys.*, 134 (2012) 1121.
41. S.F. Bdewi, O.G. Abdullah, B.K. Aziz and A.A.R. Mutar, *J. Inorg. Organomet. Polym. Mater.*, 26 (2016) 326.
42. O.G. Abdullah, Y.A.K. Salman and S.A. Saleem, *Phys. Mater. Chem.*, 3 (2015) 18.
43. G.D. Cody, T. Tiedje, B. Abeles, B. Brooks and Y. Goldstein, *Phys. Rev. Lett.*, 47 (1981) 1480.
44. S.B. Aziz, R.T. Abdulwahid, M.A. Rasheed, O.G. Abdullah and H.M. Ahmed, *Polymers*, 9 (2017) 486.
45. A.A. Ebnalwaled and A. Thabet, *Synthetic Met.*, 220 (2016) 374.
46. O.G. Abdullah and S.A. Saleem, *J. Electron. Mater.*, 45 (2016) 5910.
47. S.H. Wemple and M. Didomenico, *Phys. Rev. B*, 3 (1971) 1338.
48. A. Benchaabane, Z.B. Hamed, F. Kouki, M.A. Sanhoury, K. Zellama, A. Zeinert and H. Bouchriha, *J. Appl. Phys.*, 115 (2014) 134313.
49. O.G. Abdullah, S.B. Aziz and M.A. Rasheed, *J. Mater. Sci. Mater. Electron.*, 28 (2017) 4513.
50. S. El-Sayed, K.H. Mahmoud, A.A. Fatah and A. Hassen, *Physica B*, 406 (2011) 4068.
51. Y.B. Taher, A. Oueslati and M. Gargouri, *Ionics*, 21 (2015) 1321.
52. O.G. Abdullah, S.B. Aziz and M.A. Rasheed, *Ionics*, 24 (2018) 777.
53. M.M. El-Nahass, H.M. Zeyada, M.M. El-Samanoudy and E.M. El-Menyawy, *J. Phys. Condens. Matter*, 18 (2006) 5163.

54. O.G. Abdullah, S.B. Aziz, D.R. Saber, R.M. Abdullah, R.R. Hanna and S.R. Saeed, *J. Mater. Sci. Mater. Electron.*, 28 (2017) 8928.
55. A.M. El Sayed, H.M. Diab and R. El-Mallawany, *J. Polym. Res.*, 20 (2013) 255.
56. S.B. Aziz, M.A. Rasheed and Z.H.Z. Abidin, *J. Electron. Mater.*, 46 (2017) 6119.
57. K. Funke, *Prog. Solid State Chem.*, 22 (1993) 111.
58. A. Kahouli, A. Sylvestre, F. Jomni, B. Yangui and J. Legrand, *J. Phys. Chem. A*, 116 (2012) 1051.
59. V. Krishnakumar and G. Shanmugam, *Ionics*, 18 (2012) 403.
60. J. Sheng, H. Chen, B. Li and L. Chang, *Appl. Phys. A*, 110 (2013) 511.
61. T.A. Hanafy, *J. Appl. Polym. Sci.*, 108 (2008) 2540.
62. A. Dutta, T.P. Sinha, P. Jena and S. Adak, *J. Non-Cryst. Solids*, 354 (2008) 3952.
63. R. Baskaran, S. Selvasekarapandian, N. Kuwata, J. Kawamura and Y. Hattori, *Mater. Chem. Phys.*, 98 (2006) 55.
64. K. Mohamed, T.G. Gerasimov, F. Moussy and J.P. Harmon, *Polymer*, 46 (2005) 3847.

© 2018 The Authors. Published by ESG (www.electrochemsci.org). This article is an open access article distributed under the terms and conditions of the Creative Commons Attribution license (<http://creativecommons.org/licenses/by/4.0/>).